Istanbul Bridge Conference
August 11-13, 2014
Istanbul, Turkey

STRENGTH AND DEFORMATION CHARACTERISTICS OF ECC LINK SLAB IN JOINT-FREE BRIDGE DECKS

K.M.A. Hossain[1] and M.S. Anwar[2]

ABSTRACT

The expansion joints are a major source of deterioration of multi-span bridges in Canada and North America. Expansion joints can be replaced by flexible link slabs forming a joint-free bridge. The high strain capacity while maintaining low crack widths makes engineered cementitious composite (ECC) an ideal material for the link slab construction. The use of ECC link slab in joint free bridge construction is an emerging technology and very few research has been conducted to date on this novel form of construction. This paper presents the results of an experimental investigation on behaviour of ECC link slabs subjected monotonic loading. The performance of link slabs made with different types of ECC compared to their normal concrete (NC) counterparts is described based on load-deformation response, crack development, stiffness degradation and energy absorbing capacity.

[1]Associate Professor, Dept. of Civil Eng., Ryerson University, 350 Victoria St., Toronto, M5B 2K3, Canada
[2]Research Assistant, Dept. of Civil Eng., Ryerson University, 350 Victoria Street, Toronto, M5B 2K3, Canada

Istanbul Bridge Conference
August 11-13, 2014
Istanbul, Turkey

Strength and Deformation Characteristics of ECC Link Slab in Joint-free Bridge Decks

K.M.A. Hossain[2] and M.S. Anwar[2]

ABSTRACT

The expansion joints are a major source of deterioration of multi-span bridges in Canada and North America. Expansion joints can be replaced by flexible link slabs forming a joint-free bridge. The high strain capacity while maintaining low crack widths makes engineered cementitious composite (ECC) an ideal material for the link slab construction. The use of ECC link slab in joint free bridge construction is an emerging technology and very few research has been conducted to date on this novel form of construction. This paper presents the results of an experimental investigation on behaviour of ECC link slabs subjected monotonic loading. The performance of link slabs made with different types of ECC compared to their normal concrete (NC) counterparts is described based on load-deformation response, crack development, stiffness degradation and energy absorbing capacity.

Introduction

Billions of dollars are spent every year to repair and maintenance bridges in North America. The poor durability of concrete bridges throughout Canada is a concern for transportation

[1]Associate Professor, Dept. of Civil Eng., Ryerson University, 350 Victoria St., Toronto, M5B 2K3, Canada
[2]Research Assistant, Dept. of Civil Eng., Ryerson University, 350 Victoria Street, Toronto, M5B 2K3, Canada

authorities. With decreasing budget allocations for infrastructure maintenance, rehabilitation, and replacement, the need for greater durability is superficial. High strength concrete has been used in maintenance and repair works of infrastructures such as bridge decks with different degrees of success [1,2]. But none of these solutions target the inherent shortfall of concrete brittleness, which results in cracking. These cracks, allow salt water to contact the reinforcing bars and causing corrosion and finally leading to structural failure. A major source of bridge deterioration requiring constant maintenance is mechanical expansion joints installed between adjacent simple bridge decks [3]. A possible approach to alleviate this problem is the elimination of mechanical deck joints in multi-span bridges. Two solutions to eliminate deck joints are proposed [4-6]. First solution is an integral construction concept with girder continuity and second solution is a joint-less bridge deck concept using link slab with simply supported girders (Fig.1).

The section of the deck connecting the two adjacent simple-span girders is called the link slab (LS). Fig. 2 shows the components of a typical link slab. The length of the debond zone (throughout which all shear connectors are removed and a debonding mechanism is placed on the top flange of the girder) is 5.0% of each adjacent bridge span. It was found necessary to extend the length of the link slab 2.5% further into each adjacent span to help transfer load from the girders into the link slab through additional shear connectors. Within the extended zone, known as the transition zone, the number of shear connectors should be 50% more than the number required by AASHTO design procedures. Caner and Zia experimentally analyzed the performance of joint-free bridge decks and proposed design methods for the conventional concrete link slab [7-8].

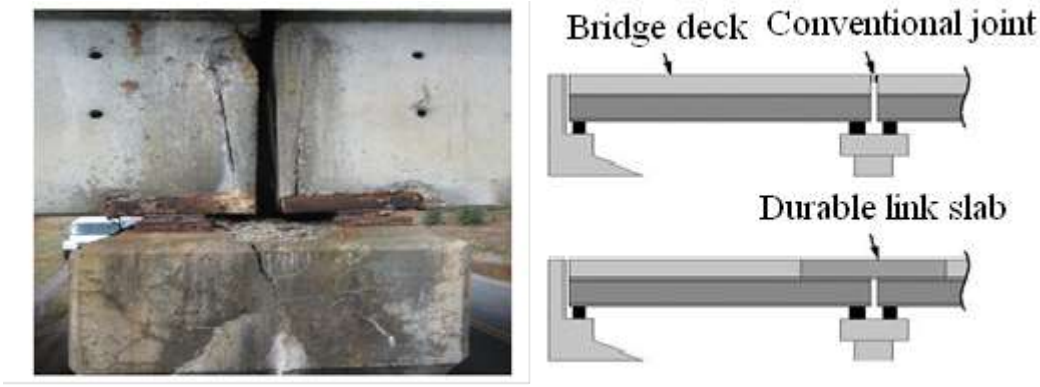

(a) Bridge deck with joint (b) Bridge deck with link slab

Figure 1. Joint-free bridge deck with link slab

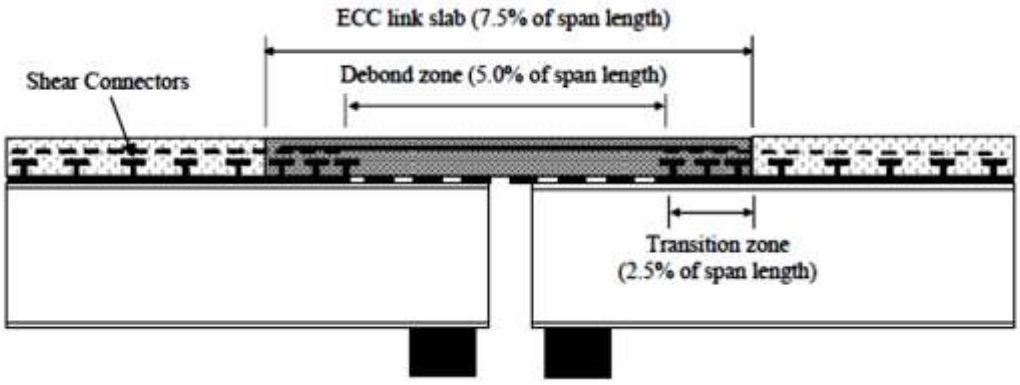

Figure 2. Schematic of ECC link slab showing components

Engineered cementitious composite (ECC) represents a new generation of high-performance concrete material that offers significant potential to naturally resolving the durability problem of reinforced concrete structures [1,2,9]. Micromechanical design of ECC allows optimization of the composite for high performance, resulting in extreme tensile strain capacity while minimizing the amount of reinforcing fibers, typically less than 2% by volume. Unlike ordinary cement-based materials, ECC strain-hardens after first cracking, similar to a ductile metal, and demonstrates a strain capacity 300 to 500 times greater than normal concrete. Even at large imposed deformation, crack widths of ECC remain small, less than 60 μm.

One approach to reducing the cement volume and in turn environmental impact of concrete has been the use of supplementary cementitious materials (SCMs) such as fly ash, volcanic ash, volcanic pumice (VP) powder etc. [10](Hossain 2013). Partial replacement of cement by SCMs improves the fresh and durability properties, reduces the drying shrinkage and matrix toughness and improves the robustness of ECC in terms of tensile ductility while decreasing environmental impacts. Benefits of using SCMs, in particular, volcanic ash or ground volcanic pumice include reductions in energy consumption, greenhouse gas releases, and other pollutant emissions from initial mining of limestone, calcinations, and grinding in cement production. Comprehensive research has been conducted over the years on ECC incorporating SCMs such as fly ash, slag, metakaolin [11-14]. Recently, author is conducting research to produce ECC by using volcanic materials as replacement of cement.

The high strain capacity while maintaining low crack widths of ECC make it an ideal material for the link slab application [[15-16]. Few research studies conducted to date showed significant enhancement of ductility and crack width control in ECC link slabs confirming that the use of ECC can be effective in extending the service life of bridge deck systems [17]. Lack of research studies warrants extensive research investigations on structural performance of ECC based link slabs [18]. The full understanding of the behaviour of ECC link slabs is very important for this new technology to be adopted in bridge structures. The use of local crushed sand and ground pumice as replacement of silica sand and cement, respectively can reduce the cost of ECC.

This paper presents the structural performance of ECC link slabs (made with finely ground volcanic pumice, fly ash, silica sand and crushed sand) compared to their conventional normal concrete (NC) counterparts based on load-deflection response, crack development, strain characteristics, energy absorbing capacity and failure modes.

Experimental Investigations

Comprehensive research consisting of experimental and theoretical investigations is in progress to study the structural performance of link slab with ECC of different types and varying geometric/material parameters under monotonic and fatigue loading conditions. Experimental results of link slabs made with four different ECC mixtures (fly ash ECC with crushed sand ‘FA-CS-ECC’, fly ash ECC with silica sand ‘FA-SS-ECC’, ground pumice ECC with crushed sand ‘VP-CS-ECC’ and ground volcanic pumice ECC with silica sand (VP-SS-ECC), and a conventional NC tested under monotonic loading condition are the subject matter of this paper.

Link Slab Configuration, Test Specimens, Material Properties and Casting

The deformed shape and moment distribution due to applied load of a two-span bridge structure with link slab (including an enlarged view of the link slab portion) are schematically

shown in Fig. 3. Flexural crack formation was expected at the top of the link slab as shown in Fig. 3.

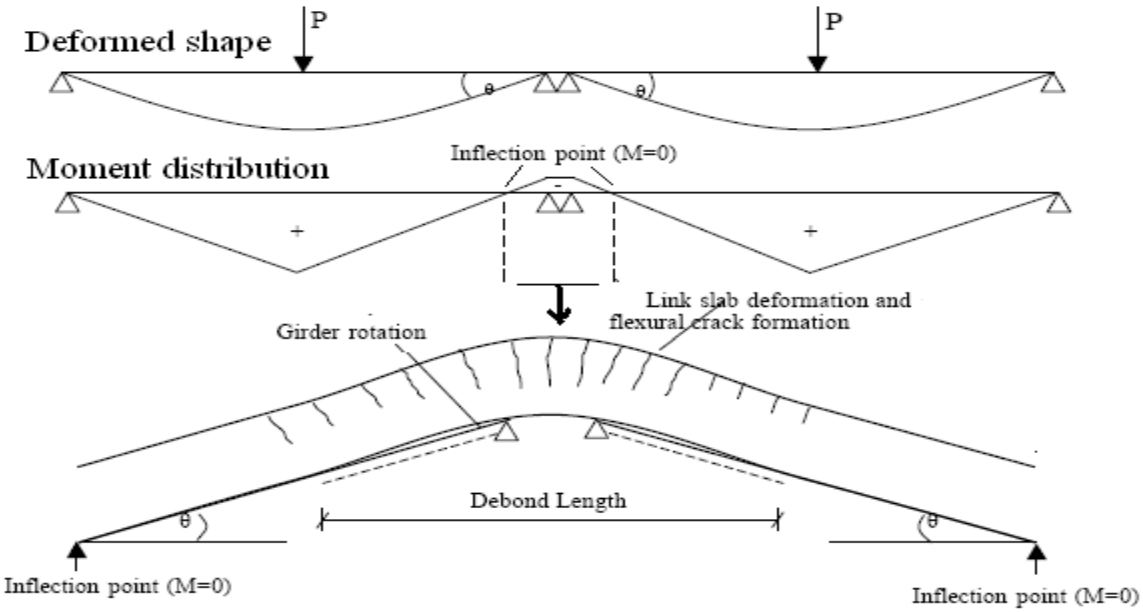

Figure 3. Two span bridge illustrating link slab deformation (between inflection points)

Therefore, the link slab specimens were designed to include the link slab within the distance between the points of inflection in the adjacent spans. The location of inflection point (depending on the stiffness of the link slab) varies between 0 and 20% of the span length, for the current study - 6.7% was selected. The design procedure for the link slab detail currently requires a debond length of 5% of the simply supported span [8] and as such, the same debond length was adopted in current study. This debond length requirement was supported by early study [6].

The testing was focused on the link slab portion between the points of inflection in the adjacent spans as illustrated in Fig. 3. Model link slab specimens of $1/4^{th}$ scale were tested. The dimensions of the representative full-scale bridge deck were 711 mm (width) and 230 mm (depth). Based on this, a typical ¼ scale link slab model had a total length of 930 mm, width of 175 mm and depth of 60 mm. Fig. 4 shows the ECC link slab specimen geometry showing debond zone length (330 mm) equal to roughly 2.5% of both adjacent spans. Fig. 4 also shows dimensions and reinforcement details of model specimens. Longitudinal reinforcements in the form of three 6 mm bars (reinforcement ratio of 0.01%) were provided. Transverse reinforcements were provided with 6 mm bars at 210 mm c/c. Eight 10 mm shear studs were installed in two rows at each end of the steel I-beam connecting concrete deck.

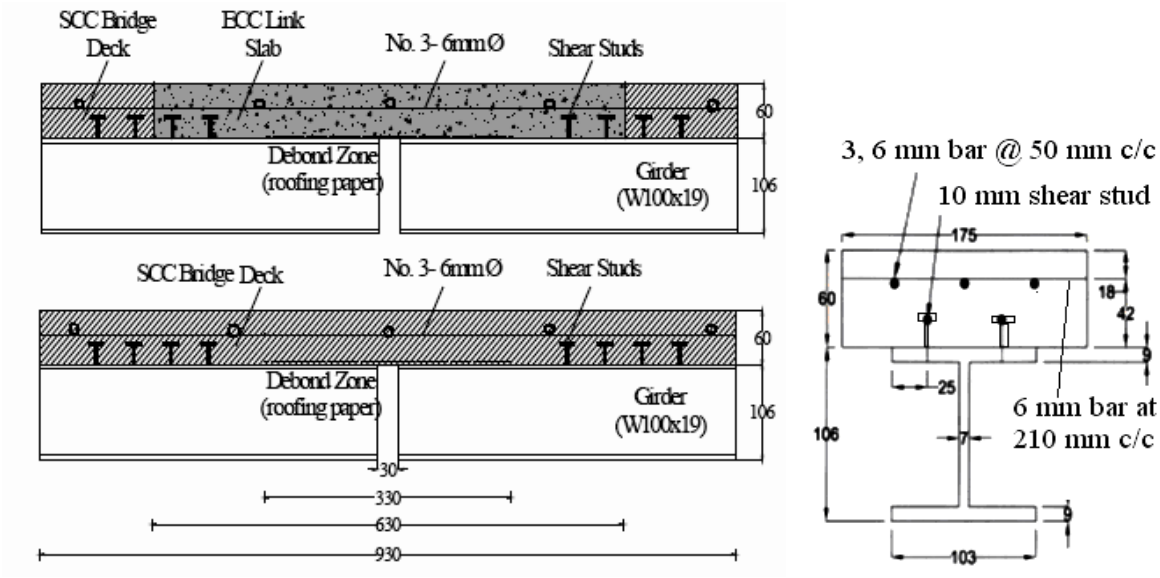

Figure 4. Geometry and reinforcement details of link slab specimens (Dimensions in mm)

Mix designs of NC and four ECC mixtures (used to make link slab specimens) are presented in Table 1. The materials used in the production of ECC mixtures were Type 10 Portland cement (ASTM Type I), ground volcanic pumice (VP), silica sand with 110 μm average grain size, locally available crushed sand with 1.18 mm maximum grain size, polyvinyl alcohol (PVA) fibers (with a diameter of 39 μm and a length of 8 mm) and a polycarboxylic-ether type high-range water-reducing admixture (HRWRA). NC was produced from Type 10 Portland cement (ASTM Type I), coarse aggregate with maximum size of 8 to 10 mm and well graded sand. The Blaine fineness ground VP was 290 m^2/kg. Ground VP satisfied the requirement of Class F fly ash as per ASTM C618.

For all link slab specimens, adjacent bridge decks (end parts) were cast with NC. For control NC link slab specimens (LS-NC), link slab portion was cast with NC. For ECC link slab specimens (designated as LS-FA-CS-ECC, LS-FA-CS-ECC, LS-VP-SS-ECC and LS-VP-CS-ECC), link slab portion was cast with four types of ECC. The details of link slab specimens are presented in Table 2.

Table 1. Mix designs of NC and ECCs

NC ingredients, kg/m^3					
Cement	Slag	Water	Coarse aggregate (lime stone)	Fine aggregate (concrete sand)	
400	90	172	810	860	
FA-SS-ECC ingredients, kg/m^3					
Cement	Fly ash	Water	PVA fiber	Silica sand	HRWRA
386	847	327	26	448	4.1
FA-CS-ECC ingredients, kg/m^3					
Cement	Fly ash	Water	PVA fiber	Crushed sand	HRWRA
386	847	327	26	428	4.1
VA-SS-ECC ingredients, kg/m^3					
Cement	Ground pumice	Water	PVA fiber	Crushed sand	HRWRA

386	645	327	26	448	4.2
VP-CS-ECC ingredients, kg/m^3					
Cement	Ground pumice	Water	PVA fiber	Crushed sand	HRWRA
386	645	327	26	428	4.2

Table 2. Dimensions and material composition on different parts of link slab (LS)

Link slab Designation	Length mm	Debond zone length (2.5%) mm	Transition zone length (2.5%) mm	Concrete type	
				Transition zone	Debond zone
LS-ECC*	930	330	150	NC	ECC
LS-NC	930	330	150	NC	NC
*LS-S-CS-ECC, LS-FS-SS-ECC, LS-VP-CS-ECC, LS-VP-SS-ECC					

For all the link slabs, as followed in the general field practice, the bridge deck part was cast initially and left for setting for 24 hours. After 24 hours, the link slab zone was cast with ECC or NC. Control specimens in the form of cylinders and beams were also cast at the same time. The specimens were cured for 28 days at the laboratory conditions while covered with burlap. The relative humidity (RH) and the temperature of the laboratory were 45 ± 5% and 24 ± 2°C, respectively. Fig. 5 shows link slab specimens during casting and after casting.

The mean yield strength, ultimate strength and modulus of elasticity of 6 mm bar are 407 MPa, 550 MPa and 224 GPa, respectively. The mean compressive strength of FA-CS-ECC, FA-SS-ECC, VP-CS-ECC, VP-SS-ECC and NC are 46 MPa, 48 MPa, 42 MPa, 40 MPa and 48 MPa, respectively while the mean flexural strength are 7.1 MPa, 7.0 MPa, 6.7 MPa, 6.5 MPa and 5.1 MPa, respectively at the age of testing.

Figure 5. Link slab specimens after casting

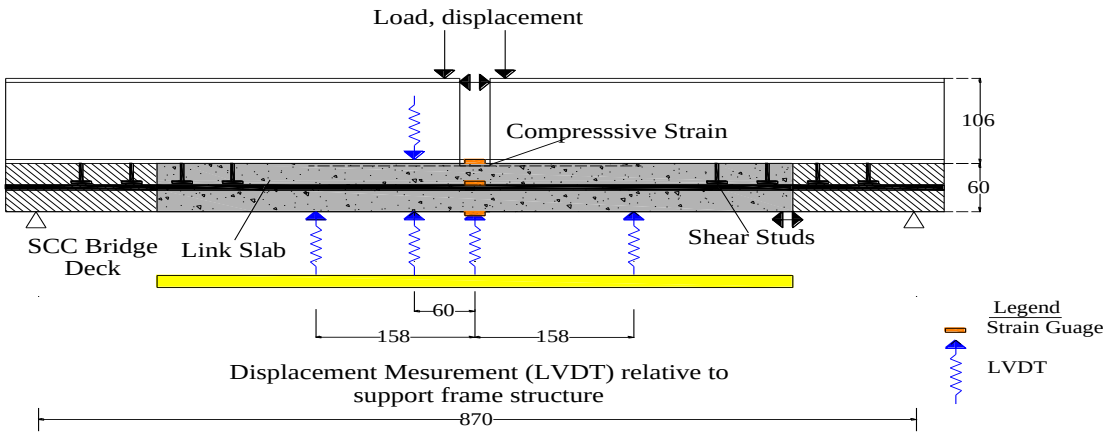

Figure 6. Test-setup and instrumentation of specimen (Dimensions in mm)

Test Set-up, Instrumentation and Testing

The link slab specimens were tested under monotonic loading simulating actual loading and support conditions of the real bridge structure. The test set-up and instrumentation of the link slab showing location of LVDT's and strain gauges are shown in Fig. 6. The test specimen was 930 mm long and supported symmetrically on roller and pin, 870 mm apart. The steel I-girders were separated by a gap of 30 mm at the centre line of the link slab. The stain gauges were installed at the centre of the specimen to monitor the strain development in concrete and reinforcing bars.

The load was applied through a hydraulic actuator at the centre of the test specimen gradually at a rate of 0.05 kN⁄min until failure (Fig. 6). The data was collected with a data acquisition system connected to computer. During testing, the load, displacements and strains in concrete and reinforcing steel of the specimens were monitored. The cracking, crack propagation and failure modes were also visually observed; simultaneously number of cracks and crack width were also noted with the help of crackscope.

Results and Discussion

Load-deflection Response, Crack Development and Failure Modes

For NC link slab (LS- NC), a small transverse crack was formed near the mid-span of the link slab at the initial loading phase. The mid-span deflection increased with the increase of load. The crack at the centre gradually grew wider and propagated across the depth to the top of the slab during subsequent loading and led to the failure (Fig. 7).

In contrast, micro-cracks appeared in at the centre of all ECC link slabs in the initial loading stages. With the increase of load, additional hairline micro-cracks formed and propagated across the length of the link slab (Fig. 7). All the crack widths remained below 50 μm and the localization of the crack near the mid-span resulted in the failure of the link slab. Just before the failure of the specimen, the ductile behavior of ECC link slabs was visually observed from the deflected shape. On the other hand, NC link slab showed failure with the formation and propagation of mainly one big crack at the centre. It was also observed that no hairline or micro-crack was formed in the region of transition zone at each side of ECC link slabs.

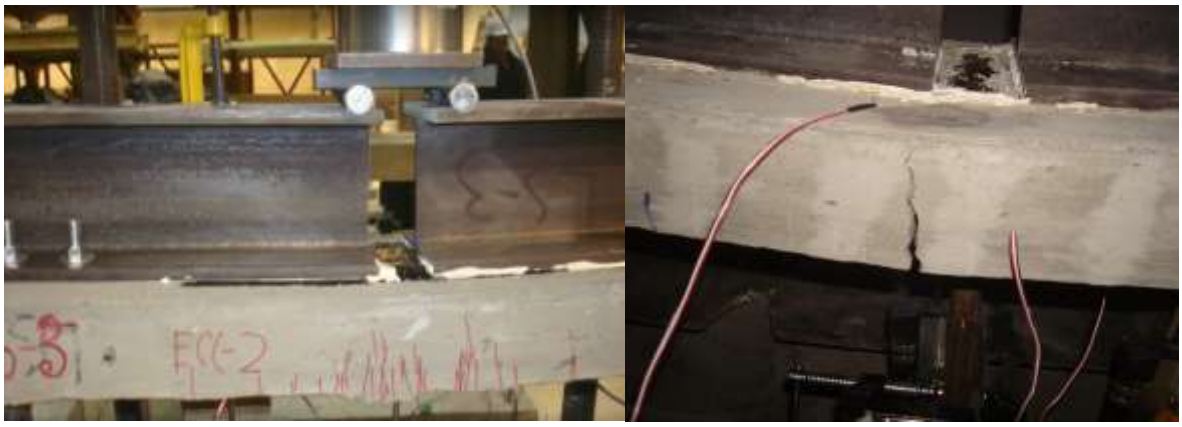

Micro-cracks in LS-VAECC Single crack in LS-NC

Figure 7. Crack propagation and failure of link slab specimens

For all the specimens including both NC and ECCs the cracks generally extended across the entire slab width indicating that the link slab behaved as a flexural member. All the cracks were observed in the debonding zone only and no crack was extended into the deck slab or in the transition zone. This provided with the evidence that the 5% debonding zone was sufficient to keep the stress concentration in the link slab only.

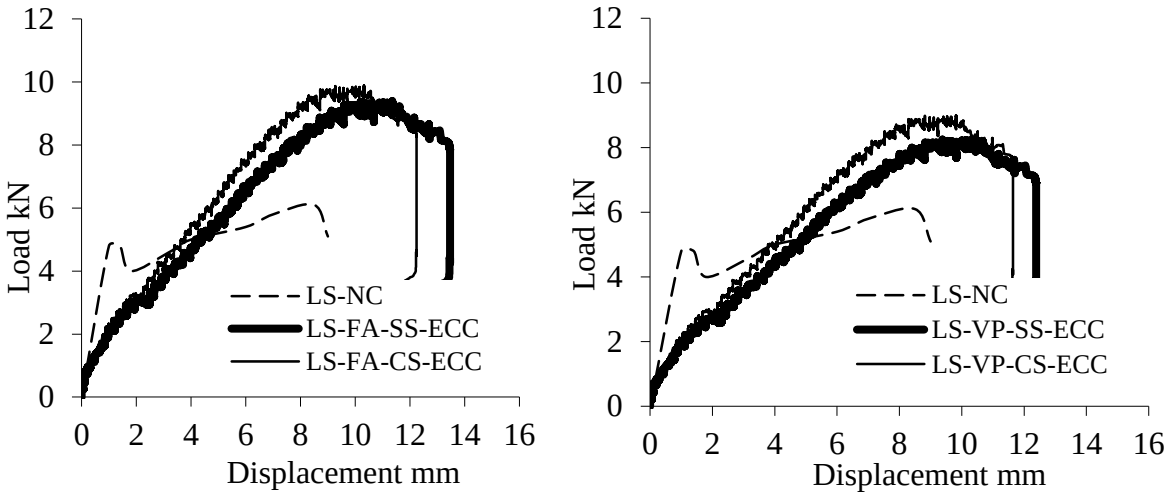

Figure 8. Comparison of load-displacment responses of NC and ECC link slabs

Fig. 8 compares the load-midspan displacement responses of NC and ECC link slab specimens. Significant differences in the responses were observed. For all ECC link slabs, the load-deflection response clearly showed ductile behaviour with strain hardening as evident from the steady increase in deformation with the increase in load. The link slab with NC failed to show similar strain hardening behaviour. During the loading history, a sudden drop of load was observed at the first peak followed by the formation of a major crack at the centre in the debonding zone (Fig. 8). The load then increased until a second peak was reached with additional deflection. This post-first peak response with large crack width may be associated with the transfer of load to the steel reinforcement (bridging the crack) through steel-NC bond mechanism. The post first peak response in NC link slab associated with single crack formation and large crack width is not acceptable for the link slab application.

Strength, Strain Hardening and Energy Absorbing Capacity

Table 3 summarizes the data depicted from load displacement responses. The ultimate load of all ECC link slabs (> 9kN) is much higher than that of NC (first peak of 4.8 kN and 2nd peak 6.14 kN). Based on the first peak, NC link slab shows significantly lower load and displacement than its ECC counterparts. Based on the first peak, the ductility (strain hardening capacity) of the ECC links slab is significantly higher as evident from the large deflection of greater than 9.81 mm compared to only 1.93 mm of NC. The energy absorbing capacity of ECC link slabs (calculated by the area under the load-deflection curve) was greater than 101 joules compared to 56 joules of its NC counterpart. While in terms of cracking, ECC link slab developed greater than 42 micro-cracks compared to one major crack in NC link slab. Link slabs with crushed sand showed higher ultimate load and energy absorbing capacity but lower peak deflection compared to their silica sand counterparts. On the other hand, link slabs with VP based ECC exhibited lower ultimate (peak) load, lower

peak deflection and lower energy absorbing capacity compared to their fly ash counterparts. Overall, performance of all ECC based link slabs is comparable and satisfactory.

Table 3: Strength, strain hardening/ductility and energy absorbing characteristics

Link slab designation	Load (1st crack)) kN	Deflection (1st crack) mm	Ultimate load kN	Ultimate Deflection mm	No. of crack	Energy Joule
LS-NC	4.66	1.93	4.8* (6.54)**	0.8* (15.0)**	1	56
LS-FA-SS-ECC	2.83	1.94	9.4	11.35	52	117
LS-FA-CS-ECC	2.94	1.82	9.9	10.32	46	121
LS-VP-SS-ECC	2.76	1.98	9.0	10.44	44	101
LS-VP-CS-ECC	2.83	1.84	9.3	9.81	42	106

*First peak ** 2nd peak

Strain Development

Load-steel strain response of the NC link slab in Fig. 9 shows sudden transfer of load to steel reinforcement at the onset of major crack development at the centre (at first peak) and subsequent large strain (stress) development in steel at lower load compared to its ECC counterpart. Such stress concentrations in the reinforcement are nonexistent even as the VA-ECC was experiencing micro-crack damage. Subsequently, the yielding of the rebar occurred at higher load in the ECC matrix compared with that in the NC matrix which is evident from the strain development in rebar (Figs. 9).

Steel strain development was higher in silica sand based ECC link slabs compared to their crushed sand counterparts. The lower steel strain development and higher ultimate load of crushed sand based ECC can be associated with the better crack resistance and aggregate interlock mechanism at the cracked surface. In addition, the superior strain hardening capacity of ECC link slabs can be attributed to the absence of shear lag between reinforcing bars and the surrounding ECC while the fracture of NC causes unloading of concrete and transfer of load to the reinforcement resulting in high interfacial shear/bond forces causing failure. Overall, VP and FA based ECC link slabs showed comparable steel strain development.

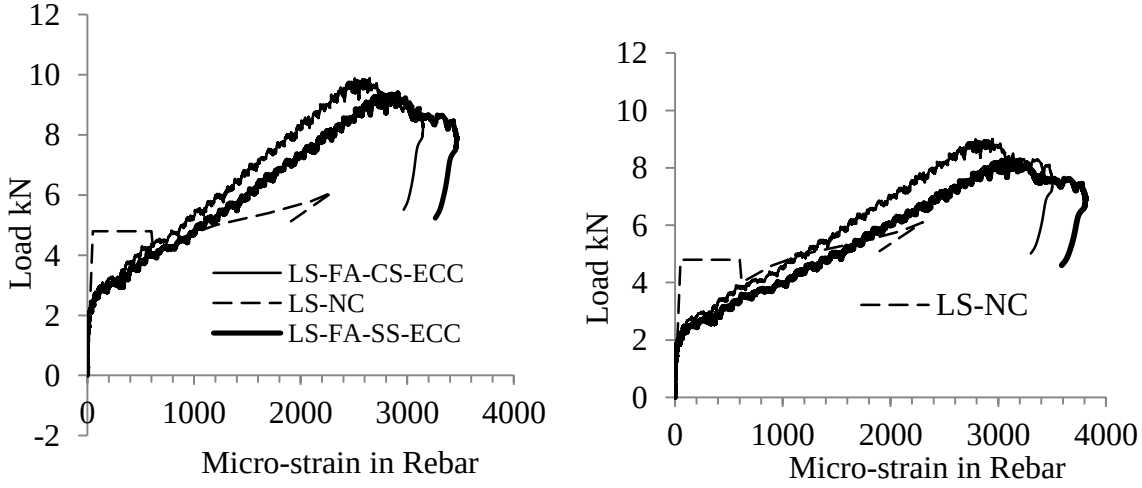

Figure 9. Load-steel strain development in link slabs

CONCLUSIONS

This paper compares the structural performance of link slabs (for joint-free bridge decks) made with four types of engineered cementitious composites (ECCs) (using combinations of ground volcanic pumice 'VP', fly ash 'FA', silica sand and crushed sand) and a conventional normal concrete (NC). Test were conducted on small-scale link slab model specimens of 1/4th scale. The following conclusions are drawn from the study:

- All ECC link slabs exhibited superior strain hardening behaviour over NC link slab. The inferior strain hardening capacity of NC link slab can be attributed to the brittle fracture of NC causing high interfacial shear and subsequent steel-concrete interfacial bond forces. This resulted in higher strain in the rebars in NC link slab (at lower load level) compared to its ECC counterparts. On the other hand, formation of micro-cracks in ECCs due to bridging action of fibers reduces rebar strain leading to stable strain hardening behaviour suitable for link slab applications.
- ECC link slab showed better performance in terms of higher ultimate strength, higher ductility, better energy absorption capacity, large number of micro-crack formation and small crack width development compared with its NC counterpart.
- Link slabs with crushed sand showed higher ultimate load and energy absorbing capacity compared to their silica sand counterparts. Link slabs with VP based ECC developed lower ultimate load and energy absorbing capacity compared to their fly ash counterparts. Overall, performance of all ECC based link slabs is comparable and satisfactory.

The study confirmed the viability of constructing link slabs using ground pumice (as cement replacement in place of fly ash) and local crushed sand (as replacement of silica sand) based ECCs to construct cost-effective sustainable joint-free bridge decks with satisfactory structural performance.

References

1. Li V.C. Engineered cementitious composites (ECC) - A review of the material and its applications. *Journal of Advanced Concrete Technology 2003;* 1(3): 215–230.
2. Li. V. C., Wang S., Ogawa A., Saito T. Interface tailoring for strain-hardening PVA-ECC. *ACI Materials Journal 2002*; 99(5):463–472.
3. Wolde-Tinsae A. M., Klinger J. E. Integral bridge design and construction. Report FHWA/MD-87/04 1987; *Maryland Department of Transportation*, USA.
4. Alampalli S., Yannotti A. P. In-service performance of integral bridges and joint less decks. *Transportation Research Record 1998;* 1624, Paper No. 98-0540, 1-7.
5. Gilani A. Link slabs for simply supported bridges incorporating cngineered cementitious composites. MDOT SPR-54181. *Structural Research Unit, 2001, MDOT*, USA.
6. Zia P., Caner A. and El-Safte A. Jointless bridge decks research project 23241-94-4. *Center for Transportation Engineering Studies 1995*; North Carolina State, pp. 1-117.
7. Caner A., Zia P. Behavior and design of link slabs for joint less bridge decks. *PCI Journal 1998;* 43: 68–80.
8. Lepech M. D., Li, V. C. , (2009), Application of ECC for bridge deck link slabs. *RILEM Journal of Materials and Structures 2009;* 42(9): 1185-1195.
9. Li V.C., Kanda T. Engineered cementitious composites for structural applications. *ASCE J. Materials in Civil Engineering 1998*, 10(2):66-69.
10. Hossain K.M.A. Effect of air entrainment and volcanic ash on the properties of self-consolidating concrete. *European Journal of Scientific Research 2013:* 95(3): 387-399.

11. Ozbay E.M., Lachemi M., Karahan O., Hossain K.M.A., Atis C.D. Investigation of the properties of ECC incorporating high volumes of fly ash and Mmtakaolin. *ACI Materials Journal 2012:* 109(5): 565-571.
12. Ozbay E.M., Karahan O., Lachemi M, Hossain K.M.A., Atis C.D. Dual effectiveness of freezing–thawing and sulfate attack on high-volume slag-incorporated ECC. *Composites Part B: Engineering 2013;* 45(1):1384-1390.
13. Şahmaran M., Lachemi M., Hossain K.M.A., Li V.C. Influence of aggregate type and size on the ductility and mechanical properties of ECC. *ACI Materials Journal 2009;* 106 (3): 308-316.
14. Wang S., Li, V.C. Engineered cementitious composites with high-volume fly ash. *ACI Materials Journal 2007;* 104(3): 233-241.
15. Sahmaran M., Lachemi M., Hossain K.M.A., Ranade R., Li, V.C. Internal curing of ECCs for prevention of early age autogenous shrinkage cracking. *Cement Concrete Research 2010*, 39(10): 893-901.
16. Fischer G., Li V. C. Design of cngineered cementitious composites (ECC) for processing and workability requirement, *BMC 2003;* Poland, 7: 29–36.
17. Keoleian G., Kendall A., Chandler R., Helfand G., Lepech M., Li, V.C. Life cycle model for evaluating the sustainability of bridge decks. *Proc. 4th Int. Workshop on Life-Cycle Cost Analysis and Design of Civil Infrastructure Systems*, Florida, May 8-11, 2005.
18. Hossain K.M.A., Maulin, B.M., Anwar, M.S. Properties and structural performance of engineered cementitious composites with special reference to bridge applications. Research Report No. STR-01, 2012, Department of Civil Engineering, Ryerson University, Toronto, Canada, 45p.